the incidence of pneumonia may have been relatively lower in such a large heterogeneous study sample.

Regarding the risk factors associated with the development of pneumonia, some of them were reported to be age, primary disease, consciousness disorders, nutritional status, poor ADL, poor oral status, and swallowing dysfunction (40, 41). In the present study, among the analysed predictors, the 'aspiration of saliva' detected by VE was the only significant risk factor for pneumonia. In cases of bad oral health, saliva contains numerous bacteria. Therefore, patients with silent aspiration of saliva (without a cough reflex) are aspirating bacteria, which may be the main factor responsible for increasing the risk of pneumonia.

Additionally, even with the elaborative feeding therapy provided in this study, the control of aspiration of saliva or silent aspiration of saliva was generally difficult. In the present study, there was also a tendency for there to be a higher incidence of pneumonia in poor ADL patients. Langmore *et al.* (42) also reported that severely dependent functional status was an especially potent predictor of aspiration pneumonia. Riquelme *et al.* (40) reported that there was a significant relationship between the ADL and mortality rate. It was also observed that patients with a BMI < 18·5 had a higher tendency to develop pneumonia ($P = 0{\cdot}070$) compared with those with a poor ADL ($P = 0{\cdot}769$). It is well known that a lower nutrition condition affects the host immunological function, thus making the subjects more susceptible to pneumonia (43).

On the other hand, aspiration of saliva was also detected as a significant risk factor for body weight loss in this study. This finding could be explained by the possible presence of subclinical aspiration-related pneumonia in those subjects with a body weight loss of 3% or more.

The overall findings in this study demonstrated that it is still very difficult to prevent aspiration of saliva even if physicians provide elaborative feeding therapy and even if patients do not eat and drink anything through the mouth. Effective strategies to prevent the silent aspiration of saliva will therefore be an important target for future research.

Conclusion

The results of this study showed that, even with elaborative feeding therapy, 'aspiration of saliva' as detected by videoendoscopic examination was found to be a significant risk factor for pneumonia and a body weight loss of 3% or more in elderly patients living in nursing homes.

Acknowledgments

The authors gratefully acknowledge Dr. Minakuchi H who helped supervise statistical analysis of the data and Dr. Hara ES who provided English editing support. This study was supported by a Research Grant for Longevity Science (22-2) from the Ministry of Health, Labour and Welfare, Japan (2010).

References

1. Ekberg O, Feinberg MJ. Altered swallowing function in elderly patients without dysphagia: radiologic findings in 56 cases. AJR Am J Roentgenol. 1991;156:1181–1184.
2. Sheth N, Diner W. Swallowing problems in the elderly. Dysphagia. 1988;3:209–215.
3. Tibbling L, Gustafsson B. Dysphagia and its consequences in the elderly. Dysphagia. 1991;6:200–202.
4. Siebens H, Trupe E, Siebens A, Cook F, Anshen S, Hanauer R *et al.* Correlates and consequences of eating dependency in the institutionalized elderly. J Am Geriatr Soc. 1986;34:192–198.
5. Steele CM, Greenwood C, Ens I, Robertson C, Seidman-Carlson R. Mealtime difficulties in a home for the aged: not just dysphagia. Dysphagia. 1997;12:43–50.
6. Croghan JE, Burke EM, Caplan S, Denman S. Pilot study of 12 month outcomes of nursing home patients with aspiration on videofluoroscopy. Dysphagia. 1994;9:141–146.
7. Mann G, Hankey GJ, Cameron D. Swallowing function after stroke: prognosis and prognostic factors at 6 months. Stroke. 1999;30:744–748.
8. Teraoka F, Nishi M, Yoshizawa T, Momose M, Hirashima Y, Ichikawa T. Outcome of dysphagia in stroke patients: predictive factors for the resumption of a regular diet (in Japanese). Jpn J Rehabil Med. 2004;41:421–428.
9. Schroter-Morasch H, Bartolome G, Troppmann N, Ziegler W. Values and limitations of pharyngolaryngoscopy (transnasal, transoral) in patients with dysphagia. Folia Phoniatr Logop. 1999;51:172–182.
10. Kikutani T, Takahashi N, Fukui T, Katagiri H, Tohara T, Tamura F *et al.* Nourishment support in the nursing care facility for the elderly through implemented conferencing for feeding support (in Japanese). Jpn J Gerodontol. 2008;22:371–376.
11. Takahashi N, Kikutani T, Tamura F, Suda M, Fukui T, Katagiri H *et al.* Evaluation of tongue motor function using videoendoscopic evaluation system for patients with mastication disorders with motor dysfunction (in Japanese). Jpn J Gerodontol. 2009;24:20–27.
12. Abe R, Furuya J, Suzuki T. Videoendoscopic measurement of food bolus formation for quantitative evaluation of masticatory function. J Prosthodont Res. 2011;55:171–178.

13. Murray J, Langmore S, Ginsberg S, Dostie A. The significance of accumulated oropharyngeal secretions and swallowing frequency in predicting aspiration. Dysphagia. 1996;11:99–103.
14. Donzelli J, Brady S, Wesling M, Craney M. Predictive value of accumulated oropharyngeal secretions for aspiration during video nasal endoscopic evaluation of the swallow. Ann Otol Rhinol Laryngol. 2003;112:469–475.
15. Ota K, Saitoh E, Baba M, Sonoda S. The secretion severity rating scale: a potentially useful tool for management of acute-phase fasting stroke patients. J Stroke Cerebrovasc Dis. 2011;20:183–187.
16. Link DT, Willging JP, Miller CK, Cotton RT, Rudolph CD. Pediatric laryngopharyngeal sensory testing during flexible endoscopic evaluation of swallowing: feasible and correlative. Ann Otol Rhinol Laryngol. 2000;109:899–905.
17. Langmore SE, Schatz K, Olson N. Endoscopic and videofluoroscopic evaluations of swallowing and aspiration. Ann Otol Rhinol Laryngol. 1991;100:678–681.
18. Bastian RW. The videoendoscopic swallowing study: an alternative and partner to the videofluoroscopic swallowing study. Dysphagia. 1993;8:359–367.
19. Lim SHB, Lieu PK, Phua SY, Seshadri R, Venketasubramanian N, Lee SH *et al.* Accuracy of bedside clinical methods compared with fiberoptic endoscopic examination of swallowing (FEES) in determining the risk of aspiration in acute stroke patients. Dysphagia. 2001;16:1–6.
20. Rosenbek JC, Robbins J, Roecker EB, Coyle JL, Wood JL. A penetration-aspiration scale. Dysphagia. 1996;11:93–98.
21. Landis JR, Koch GG. The measurement of observer agreement for categorical data. Biometrics. 1977;33:159–174.
22. Crary M, Groher M (eds). The introduction to adult swallowing disorders. Woburn, MA: Butterworth-Heinemann; 2003.
23. National Dysphagia Diet Task Force. The National Dysphagia Diet: standardization for optimal care. Chicago, IL: American Dietetic Association; 2002.
24. Cabre M, Serra-prat M, Palomera E, Almirall J, Pallares R, Clave P. Prevalence and prognostic implications of dysphagia in elderly patients with pneumonia. Age Ageing. 2010;39:39–45.
25. Blackburn GL, Bistrian BR, Maini BS, Schlamm HT, Smith MF. Nutritional and metabolic assessment of the hospitalized patient. J Parenter Enteral Nutr. 1977;1:11–22.
26. Teramoto S, Fukuchi Y, Sasaki H, Sato K, Sekizawa K, Matsuse T. High incidence of aspiration pneumonia in community- and hospital-acquired pneumonia in hospitalized patients: a multicenter, prospective study in Japan. J Am Geriatr Soc. 2008;56:577–579.
27. Yamaya M, Yanai M, Ohrui T, Arai H, Sasaki H. Interventions to prevent pneumonia among older adults. J Am Geriatr Soc. 2001;49:85–90.
28. Doggett DL, Tappe KA, Mitchell MD, Chapell R, Coates V, Turkelson CM. Prevention of pneumonia in elderly stroke patients by systematic diagnosis and treatment of dysphagia: an evidence-based comprehensive analysis of the literature. Dysphagia. 2001;16:279–295.
29. Leder SB, Sasaki CT, Burrell MI. Fiberoptic endoscopic evaluation of dysphagia to identify silent aspiration. Dysphagia. 1998;13:19–21.
30. Ramsey D, Smithard D, Kalra L. Silent aspiration: what do we know? Dysphagia. 2005;20:218–225.
31. Linden P, Siebens A. Dysphagia: predicting laryngeal aspiration. Arch Phys Med Rehabil. 1983;64:281–284.
32. Logemann JA. Evaluation and treatment of swallowing disorders. San Diego: College-Hill Press; 1983.
33. Kidder TM, Langmore SE, Martin JW. Indications and techniques of endoscopy in evaluation of cervical dysphagia: comparison with radiographic techniques. Dysphagia. 1994;9:256–261.
34. Broniatowski M. Fiberoptic endoscopic evaluation of dysphagia and videofluoroscopy. Dysphagia. 1998;13:22–23.
35. Kelly A, Drinnan M, Leslie P. Assessing penetration and aspiration: how do videofluoroscope and fiberoptic endoscopic evaluation of swallowing compare? Laryngoscope. 2007;117:1723–1727.
36. Gerek M, Atalay A, Cekin F, Ciyiltepe M, Ozkaptan Y. The effectiveness of fiberoptic endoscopic swallow study and modified barium swallow study techniques in diagnosis of dysphagia. Kulak Burun Bogaz Ihtis Derg. 2005;15:103–111.
37. Tohara H, Nakane A, Murata S, Mikushi S, Ouchi Y, Wakasugi Y *et al.* Inter- and intra-rater reliability in fibroptic endoscopic evaluation of swallowing. J Oral Rehabil. 2010;33:884–891.
38. Staff DM, Shaker R. Videoendoscopic evaluation of supraesophageal dysphagia. Curr Gastroenterol Rep. 2001;3:200–205.
39. Wu CH, Hsiao TY, Chen JC, Chang YC, Lee SY. Evaluation of swallowing safety with fiberoptic endoscope: comparison with videofluoroscopic technique. Laryngoscope. 1997;107:396–401.
40. Riquelm R, Torres A, El-Ebiary M, De La Bellacasa JP, Estruch R, Mensa J *et al.* Community-acquired pneumonia in the elderly: a multivariate analysis of risk and prognostic factors. Am J Respir Crit Care Med. 1996;154:1450–1455.
41. Splaingard M, Hutchins B, Sulton L, Chaudhuri G. Aspiration in rehabilitation patients: videofluoroscopy vs bedside clinical assessment. Arch Phys Med Rehabil. 1988;69:637–640.
42. Langmore SE, Terpenning MS, Schork A, Chen Y, Murray JT, Lopatin D *et al.* Predictors of aspiration pneumonia: how important is dysphagia? Dysphagia. 1998;13:69–81.
43. Rothan-Tondeur M, Meaume S, Girard L, Weill-Engerer S, Lancien E, Abdelmalak S *et al.* Risk factors for nosocomial pneumonia in a geriatric hospital: a control-case one-center study. J Am Geriatr Soc. 2003;51:997–1001.

Correspondence: Takeshi Kikutani, Division of Oral Rehabilitation, The Nippon Dental University Graduate School of Life Dentistry, 9-20 Fujimi1-chome, Chiyoda-ku, Tokyo 102-8159, Japan.
E-mail: kikutani@tky.ndu.ac.jp

JBC Papers in Press. Published on April 19, 2010 as Manuscript M110.127027
The latest version is at http://www.jbc.org/cgi/doi/10.1074/jbc.M110.127027

PANNEXIN 3 REGULATES INTRACELLULAR ATP/cAMP LEVELS AND PROMOTES CHONDROCYTE DIFFERENTIATION

Tsutomu Iwamoto[1,2], Takashi Nakamura[1,2], Andrew Doyle[1], Masaki Ishikawa[1], Susana de Vega[1], Satoshi Fukumoto[2], and Yoshihiko Yamada[1]

[1]Laboratory of Cell and Developmental Biology, National Institute of Dental and Craniofacial Research, National Institutes of Health, Bethesda, Maryland 20892-4370, USA; [2]Department of Pediatric Dentistry, Tohoku University Graduate School of Dentistry, Sendai 980-8576, Japan

Running head: Pannexin 3 and chondrocyte differentiation
Address correspondence to: Yoshihiko Yamada, PhD. Bldg. 30, Rm. 407, NIDCR, NIH, 30 Convent Drive MSC 4370, Bethesda, MD 20892-4370. Tel: 301-496-2111; Fax: 301-402-0897; E-mail: yoshi.yamada@nih.gov

Pannexin 3 (Panx3) is a new member of the gap junction pannexin family, but its expression profiles and physiological function are not yet clear. We demonstrate in this paper that Panx3 is expressed in cartilage and regulates chondrocyte proliferation and differentiation. *Panx3* mRNA was expressed in the prehypertrophic zone in the developing growth plate and was induced during the differentiation of chondrogenic ATDC5 and N1511 cells. Panx3-transfected ATDC5 and N1511 cells promoted chondrogenic differentiation, but the suppression of endogenous Panx3 inhibited differentiation of ATDC5 cells and primary chondrocytes. Panx3-transfected ATDC5 cells reduced PTH-induced cell proliferation and promoted the release of ATP into the extracellular space, possibly by action of Panx3 as a hemichannel. Panx3 expression in ATDC5 cells reduced intracellular cAMP levels and the activation of CREB, a PKA downstream effector. These Panx3 activities were blocked by anti-Panx3 antibody. Our results suggest that Panx3 functions to switch the chondrocyte cell fate from proliferation to differentiation by regulating the intracellular ATP/cAMP levels.

Cartilage plays an important role in mechanical load resistance and in skeletal structure support. It also serves as the skeletal template for endochondrial ossification by which most bones in the body, such as long bones, are formed. In endochondral ossification, cartilage development is initiated by mesenchymal cell condensation, followed by a series of proliferation and differentiation processes. Cells undergoing condensation differentiate into chondrocytes, which then proliferate, produce type II collagen, and form the proliferative zone of the cartilage molds. As development proceeds, chondrocytes in the center of the cartilage molds (prehypertrophic zone) cease proliferating and differentiate into type X collagen-producing hypertrophic chondrocytes, to form the hypertrophic zone. Terminally differentiated hypertrophic chondrocytes mineralize the surrounding matrix. Eventually these cells die by apoptosis and are replaced by osteoblasts that form trabecular bone.

The regulation of chondrocyte proliferation and differentiation must be tightly coordinated, in order to allow formation of properly sized cartilage and bone (1). Parathyroid-hormone-related peptide (PTHrP) and parathyroid hormone (PTH) sustain chondrocyte proliferation and delay differentiation of the growth plate (2). PTHrP is expressed by perichondrial cells and chondrocytes in the upper region of growing cartilage. Mutant mice that are deficient in PTHrP (3), PTH (4), or its receptor (5) have short proliferative zones and accelerated chondrocyte differentiation, which results in abnormal endochondrial bone formation. In contrast, mice that overexpress PTHrP have enlarged proliferative zones and delayed chondrocyte terminal differentiation (6). Humans with an activating mutation in the PTH/PTHrP receptor develop Jansen's metaphyseal chondrodysplasia, characterized by

disorganization of the growth plates and delayed chondrocyte terminal differentiation (7). These results suggest that PTH/PTHrP signaling regulates skeletal development by promoting cell proliferation and inhibiting hypertrophic differentiation of chondrocytes.

The binding of PTH/PTHrP to its receptor activates both G_s and G_q family heterotrimeric G proteins (8,9). The activation of G_s is necessary for cAMP production and protein kinase A (PKA) activation, which leads to phosphorylation of the cAMP response element binding (CREB) family of transcription factors. CREB then induces genes such as the cyclin D1 and cyclin A genes. The activated cyclin/cyclin-dependent kinases in turn phosphorylate the retinoblastoma protein (pRB) and its relative factors, which then dissociates the E2F transcription factor and subsequently activates the target genes necessary for DNA replication and cell cycle progression. Thus CREB is a direct target of PKA and a downstream target of PTH/PTHrP/cAMP signaling and is required for chondrocyte proliferation (10,11). How proliferation signaling is downregulated in the prehypertrophic zone to stop proliferation and allow the switch to the postmitotic state, is not well understood.

Pannexins, relatives of innexins that had been considered as exclusively invertebrate gap junction proteins, were recently discovered as candidates for a second family of gap junction proteins in vertebrates (12). Although there are some similarities in domain structures between pannexins and connexins, which are well characterized as vertebrate gap junction proteins, these 2 protein families have no sequence homology (13). The pannexin family has 3 members: pannexin 1 (Panx1), pannexin 2 (Panx2), and pannexin 3 (Panx3). These proteins were originally identified in the human and mouse genomes (12). The expression of Panx1 is observed in many organs, such as the eye, thyroid, prostate, kidney, and liver, but its expression is especially strong in both the developing and mature central nervous system (CNS) (12-14). Panx2 is preferentially expressed in the CNS. Recently, it was reported that Panx3 is expressed in skin, cartilage, and cochlea (15-17).

In *Xenopus* oocytes, Panx1 forms both non-junctional hemichannels and intercellular channels and interacts with Panx2 (18). Panx1 hemichannels are stress-sensitive conduits for ATP (19). Panx1 is a Ca^{2+}-permeable ion channel that is localized on both the ER and plasma membrane, and participates in ER Ca^{2+} leakage and intercellular Ca^{2+} movement (20). Both Panx1 and Panx3 are glycoproteins and N-glycosylation of these pannexins plays a role in intracellular trafficking and functional channel function (15,16). The physiological function of pannexins in cell differentiation has not yet been characterized, however.

In this paper, we report that Panx3 regulates the proliferation and differentiation of chondrocytes. *Panx3* mRNA was expressed in prehypertrophic chondrocytes and induced during the differentiation of chondrogenic ATDC5 cells. The transfection of Panx3 into ATDC5 cells promoted ATDC5 cell differentiation, whereas the inhibition of endogenous Panx3 by shRNA blocked differentiation. Panx3 promoted ATP release into the extracellular space and inhibited PTH-mediated cell proliferation, intracellular levels of cAMP, and phosphorylation of CREB. Thus our results suggest that Panx3 regulates the transition of proliferation to differentiation in chondrocytes.

EXPERIMENTAL PROCEDURES

Reagents— Insulin-transferrin-sodium selenite (ITS) was obtained from Sigma. Recombinant rat PTH (1-34) was purchased from Bachem. Recombinant human BMP2 was purchased from Humanzyme.

In situ hybridization— Digoxigenin-11-UTP-labeled, single-stranded antisense RNA probes for *Panx3*, *Ihh*, *Col2a1*, *Col10a1*, and *Hist1h4c* were prepared using the DIG RNA labeling kit (Roche Applied Science) according to the manufacturer's instructions. In situ hybridization of the tissue sections was performed essentially according to the protocol provided with Link-Label ISH Core Kit (Biogenex). Frozen tissue sections from growth plates (E16.5) were generated and placed on RNase-free glass slides. After

drying the frozen sections for 10 min at room temperature and incubating at 37°C for 30 min, the sections were treated with 10 μg/ml of proteinase K at 37°C for 30 min. Hybridization was performed at 37°C for 16 h, and washes were carried out with 2x SSC at 50°C for 15 min and 2x SSC containing 50% formamide at 37°C for 15 min. The slides were then subjected to digestion with 10 μg/ml RNase A in 10 mM Tris-HCl (pH 7.6), 500 mM NaCl, and 1 mM EDTA at 37°C for 15 min and then washed. The sections were treated with 2.4 mg/ml Levamisol (Sigma) to inactivate endogenous alkaline phosphatase.

Antibody for Panx3— A rabbit polyclonal antibody to a peptide (amino acid residues, HHTQDKAGQYKVKSLWPH) from the first extracellular loop of the mouse Panx3 protein was prepared. The antiserum was purified by the peptide affinity column. This purified antibody reacts specifically to Panx3 and was used for immunohistochemistry, Western blotting, and functional blocking assay. For inhibition by the Panx3-antibody, the cells were incubated with 10 ng/ml affinity-purified antibody or control IgG for 30 min before the experiments. To abrogate the blocking activity with Panx3-antibody, the Panx3 peptide was pre-incubated with the Panx3-antibody. A peptide with a scrambled sequence (WHTKYQVGLDPQHKASHK) of the Panx3 peptide was used as a control.

Immunohistochemistry— Frozen tissue sections were fixed with acetone at -20°C for 2 min and treated with L.A.B. (Liberate Antibody Binding) solution for 15 min at 37°C. For cultured cell staining, the cells were fixed with acetone at -20°C for 2 min. Immunohistochemistry was performed on sections that were incubated with Universal Blocking Reagent (BioGenex) for 7 min at room temperature before incubation with the primary antibody. The primary antibodies were detected by Cy-3- or Cy-5-conjugated secondary antibodies (Jackson ImmunoResearch Laboratories). Nuclear staining was performed with Hoechst dye (Sigma-Aldrich). A fluorescence microscope (Axiovert 200; Carl Zeiss MicroImaging, Inc.) and 510 Meta Confocal Microscope (Zeiss) were used for immunofluorescent image analysis. For GFP and ER-Tracker Red (Invitrogen) staining, ATDC5 cells were transfected for 2 days and then stained with ER-Tracker Red as described in the manufacturer's instructions. The images were prepared with AxioVision and Photoshop (Adobe Systems, Inc.).

Cell culture— ATDC5 cells (21) were grown in Dulbecco's modified Eagle's medium/F-12 (Life Technologies, Inc.) containing 5% fetal bovine serum (HyClone) and under 5% CO_2. In proliferation conditions, cells were maintained under confluency, and the media were replaced every other day. In differentiation conditions, cells were plated in confluency and incubated in the same medium plus 10 μg/ml of insulin, 10 μg/ml of transferrin, and 10 μg of selenium. N1511 cells (22) were cultured with α-MEM (Life Technologies, Inc.) containing 2% fetal bovine serum (HyClone) under 5% CO_2. As differentiation conditions, 1 μM insulin, 100 ng/ml rhBMP2, and 50 μg/ml ascorbic acid were added in the culture medium.

Mouse primary chondrocytes were isolated from neonatal ICR mice as previously described (23). Distal cartilaginous ends of femurs and humeri were digested with 0.25% trypsin/0.01% EDTA for 15 min, followed by digestion with 2 mg/ml collagenase type I (Worthington) in DMEM/F-12 overnight. Neonatal mouse cartilage tissue was dispersed by pipetting, and cells were filtered through 100 μm cell strainers (FALCON). Single cells were inoculated onto type I collagen-coated multiwell dishes maintained in 10% FBS in αMEM.

RT-PCR and real-time PCR— Total RNA was extracted from cells using the Trizol reagent kit (Invitrogen). Two μg of total RNA was used for reverse transcription to generate cDNA, which was used as a template for PCR with gene-specific primers. Each cDNA was amplified with an initial denaturation at 95°C for 3 min; then 95°C for 30 s, 60°C for 30 s, and 72°C for 30 s for 25 cycles; and a final elongation step at 72°C for 5 min and then separated on agarose gels. Real-time PCR was performed

with SYBR Green PCR Master Mix and the TaqMan 7700 Sequencer Detection System (Applied Biosystems). PCR was performed for 40 cycles, 95°C for 1 min, 60°C for 1 min, and 72°C for 1 min. Gene expression was normalized to the housekeeping gene *S29*. The reactions were run in triplicate and repeated 3 times, and the results were combined to generate the graphs. The following primer sequences were used: *Panx3*, 5'-GCCCCTGGATAAGATGGTCAAG -3' and 5'- GCGGATGGAACGGTTGTAAGA -3'; *Panx1*, 5'-TTTGGACCTAAGAGACGGACCTG -3' and 5'-CGGGAATCAGCAGAGCATACAC -3'; *Panx2*, 5'-ACAAGGGCAGTGGAGGTGATTC -3' and 5'-CGATGAGGATAGCGTGCTGATG -3'; *Col2a1*, 5'-GAAAAACTGGTGGAGCAGCAAGAGC -3' and 5'-CAATAATGGGAAGGCGGGAGGTC -3'; *Agc1*, 5'-TGGAGCATGCTAGAACCCTCG -3' and 5'- GCGACAAGAAGACACCATGTG -3'; *Col10a1*, 5'-AGCCCCAAGACACAATACTTCATC -3' and 5'-TTTCCCCTTTCCGCCCATTCACAC -3'; *PPR*, 5'-ACTACTACTGGATTCTGGTGGAGGG -3' and 5'-CTGGAAGGAGTTGAAGAGCATCTC -3'; *PTHrP*, 5'-CAGACGATGAGGGCAGATACCTAAC -3' and 5'-CAGTTTCCTGGGGAGACAGTTTG -3'; and *Gapdh*, 5'-ACCACAGTCCATGCCATCAC -3' and 5'- TCCACCACCCTGTTGCTGTA -3'. The predicted size of each fragment is 373, 380, 442, 392, 325, 463, 470, 558, 470, 372, and 452 base pairs, respectively.

Western blotting— The cells were washed 3 times with phosphate-buffered saline containing 1 mM sodium vanadate (Na_3VO_4), then solubilized in 100 µl of lysis buffer (10 mM Tris-HCl (pH 7.4), 150 mM NaCl, 10 mM $MgCl_2$, 0.5% Nonidet P-40, 1 mM phenylmethylsulfonyl fluoride, and 20 units/ml aprotinin). Lysed cells were centrifuged at 14,000 rpm for 30 min, and the protein concentration of each sample was measured with Micro-BCA Assay Reagent (Pierce Chemical Co.). The samples were denatured in SDS sample buffer and loaded onto a 12% SDS-polyacrylamide gel. Ten µg of lysate protein was applied to each lane. After SDS-polyacrylamide gel electrophoresis, the proteins were transferred onto a polyvinylidene difluoride membrane and immunoblotted with anti-CREB, anti-phospho-CREB (Cell Signaling Technology, Inc.), anti-MAP kinase, and anti-phospho-MAP kinase (New England Biolabs) and then visualized using an ECL kit (Amersham Pharmacia Biotech). For CREB and ERK1/2 experiments, the cells were pretreated as follows: The cells ($3x10^4$ cell/cm^2) were plated in a 60 mm-dish and cultured with 10 µg/ml of insulin, 10 µg/ml of transferrin, and 10 µg of selenium for 7 days. They were incubated with serum-free 0.1% albumin-containing DMEM/F-12 medium for 8–12 h and then exposed to 100 nM rPTH (1-34) for the appropriate times.

Plasmid construction and transfection— The coding sequence of mouse Panx3 cDNA was subcloned into the pEF1/V5-His vector (pEF1/Panx3) and pcDNA3.1-GFP-TOPO (Panx3-pcDNA-GFP) (Invitrogen). As a control, an empty vector of pEF1 or was pcDNA3.1-GFP-TOPO used. ATDC5 cells or N1511 cells were transiently transfected using Nucleofector (Amaxa). Briefly, cells were resuspended in 100 µl of Nucleofector solution T and transfected with 5 µg of DNA using Program T-20. Transfection efficiency using these conditions was shown to be >70%. For stable transfection of ATDC5 cells, selection was initiated 24 h after transfection using G418 (Invitrogen) at a concentration of 600 µg/ml for 2 weeks. Pools of transfected cells were collected and cultured as the parental ATDC5 cells, in the continued presence of 60 µg/ml of G418. All experiments were performed 3 times, and representative experiments are shown. For transient transfection, Panx3-pcDNA-GFP was transfected into ATDC5 cells under the same conditions as used for stable transfection, except that G418 was omitted.

Alcian blue staining— The cells were first rinsed with PBS 3 times, and then fixed with 100% methanol for 10 min at –20°C. Staining was accomplished by applying a solution of 0.1% Alcian Blue 8 GX in 0.1 M HCl to the cells for 2 h at room temperature. To quantify the intensity of the staining, the stained culture plates were rinsed with PBS 3 times and the well extracted with 6 M guanidine/HCl for 8 h at room temperature. The optical density of the extracted dye was measured at 650 nm.

Short-hairpin RNA experiments— Panx3-specific knockdowns were performed with the expression of short-hairpin RNA (shRNA) using a pSM2 vector (Open Biosystems). The shRNA construct contains the 3'-untranslated region of *Panx3* (GGCAGGGTAGAACAATTTA). A non-silencing shRNA construct from Open Biosystems, whose sequence has been verified to contain no homology to known mammalian genes, was used as a control. The cells were transfected with shRNA plasmids using Nucleofection (Amaxa). Selection was performed 24 h after transfection with puromycin at a concentration of 4 μg/ml for 5 days.

siRNA experiments— siRNAs targeting mouse Panx3 (NM_172454) (Panx3 siRNA-1, 5'-UAAUAAGGAUGUCCACGUA-3' and Panx3 siRNA-2, 5'-GGGCUCAGAUUAUGGACUA-3') were purchased from Dharmacon. (siGenome On-Target plus; Dharmacon). Negative control siRNA duplex (Stealth RNAi negative control; invitrogen) was used as control. Forward transfection for ATDC5 cells and reverse transfection for primary chondrocytes were carried out using Lipofectamine RNAiMAX reagent (Invitrogen), according to the manufacturer's protocol. In forward transfection, ATDC5 cells were transfected with 50 nM siRNA duplex in regular serum-free culture medium without antibiotics, using Lipofectamine RNAiMAX reagent. After 8 h incubation with the transfection reagent mix, the medium was changed to the differentiation medium with BMP-2 and incubated for 8 days. In reverse transfection, freshly isolated chondrocytes were plated at an initial density of $5x10^4/cm^2$, into the plates that had been coated with Panx3 siRNA-1, siRNA-2 or Stealth RNAi negative control in the presence of Lipofectamine RNAiMAX reagent. After 8 h incubation with the transfection reagent mix, the medium was changed to the differentiation medium with BMP-2 and incubated for 2 days. Expression of *Panx3, Col2a1* and *Col10a1* were analyzed by real time PCR methods.

Measurement of intracellular cAMP— The cells were seeded at 1 X 10^4 cells/well in a 96-well plate and cultured for 7 days with DMEM/F-12 in the presence of 10 μg/ml of ITS. They were then incubated with serum-free 0.1% albumin containing DMEM/F-12 medium for 8–12 hours, followed by exposure to 100 nM rPTH (1-34) for 10 min. The level of cAMP was determined with a Bridge-It cAMP Designer Fluorescence Assay kit (Mediomics). Briefly, the cells were incubated with 50 μl of 1x KRB-IBMX buffer for 15 min at RT and with 50 μl of Forskolin for 15 min at RT. After the solution was removed, the cells were incubated with 100 μl of the cAMP designer assay solution for 30 min while covered with tinfoil to avoid exposure to light. The supernatant was collected and the fluorescence intensity was measured with a plate reader (excitation ~480–485 nm, emission ~520–535 nm).

Measurement of ATP flux

ATP flux was determined by luminometry. To open the pannexin channels, the cells were depolarized by incubation in KGlu solution (140 mM KGlu, 10 mM KCl and 5.0 mM TES, pH 7.5) for 10 min. The supernatant was collected and assayed with luciferase/luciferin (Promega).

RESULTS

Expression of Panx3 in cartilage— While searching for an expression profile of gap junction genes in skeletal tissues through the EST database, we found that *Panx3* was expressed in limbs and cartilage. Because of its unique expression profile and its potential

function in skeletal development, we characterized the expression and function of Panx3 in cartilage. In situ hybridization of the embryonic day (E) 16.5 growth plates revealed that *Panx3* mRNA was strongly expressed in the prehypertrophic zone (Fig. 1A, a). A control sense probe for *Panx3* showed no signal (Fig. 1A, b). Indian hedgehog (*Ihh*) mRNA was expressed in prehypertrophic and hypertrophic chondrocytes at this stage (Fig. 1A, c). mRNA for type II collagen (*Col2a1*), a major collagen in cartilage, was expressed in the resting, proliferative, and prehypertrophic zones (Fig. 1A, d). Type X collagen (*Col10a1*) mRNA was expressed in the prehypertrophic and hypertrophic chondrocyte chondrocytes (Fig. 1A, e). Histone H4 (*Hist1h4c*), a marker for cell proliferation, was expressed in proliferating chondrocytes (Fig. 1A, f). Immunostaining with a Panx3 antibody showed that Panx3 protein was expressed in prehypertrophic and hypertrophic chondrocytes and was localized on the surface of these cells (Fig. 1B). Panx3 was also expressed in perichondrial cells and osteoblasts.

Expression of Panx3 in differentiating chondrogenic cells— The expression of *Panx3* mRNA in a transitional stage between proliferative and hypertrophic chondrocytes suggests that Panx3 regulates chondrocyte proliferation and differentiation. To assess the role of Panx3 in chondrocyte differentiation, we used the murine chondrogenic cell lines ATDC5 and N1511, which are used to study multistep processes of chondrocyte differentiation (21),(22). ATDC5 cells proliferate until confluency, and then differentiate into chondrocytic phenotypes in a prolonged culture in the presence of insulin (21). Factors such as BMP-2, GDF-5, and TGFβ accelerate the chondrogenic differentiation of ATDC5 cells (24-26). We first examined the expression of *Panx3* mRNA during differentiation of the ATDC5 cells in the presence of insulin using real-time RT-PCR (Fig. 2A). *Panx3* mRNA expression was induced during ATDC5 cell differentiation, and reached its highest level after 20 days of culture (Fig. 2A). The expression of *Col2a1* mRNA was increased in a similar manner to that of *Panx3* mRNA; *Col10a1* mRNA was induced at later stages of differentiation. Without insulin, the induction of *Panx3*, *Col2a1*, and *Col10a1* was low even in a prolonged culture, indicating that *Panx3* expression was clearly linked to the differentiation of ATDC5 cells. We observed similar expression patterns in those genes during BMP-2-induced ATDC5 differentiation, except that BMP-2 promoted differentiation much faster than insulin (data not shown). In another chondrogenic cell line N1511, BMP-2- and insulin-induced expression of *Panx3*, *Col2a1*, and *Col10a1* were seen (Fig. 2B). Western blot analysis demonstrated that Panx3 protein with a molecular weight of 45-kDa was induced in differentiated ATDC5 cells (Fig. 2C). These results indicate that Panx3 was induced during chondrogenic differentiation of ATDC5 and N1511 cells.

Membrane localization of Panx3 in ATDC5 cells— To examine cellular localizations of Panx3, we immunostained differentiated ATDC5 cells using anti-Panx3 antibody (Fig. 2D). Panx3 was expressed in the plasma membrane, cell extensions, and in organelles most likely found in the endoplasmic reticulum (ER) and the Golgi of ATDC5 cells 8 days after differentiation induction. Panx3 was co-localized with Calnexin, an endoplasmic reticulum (ER) marker, indicating that the localization of Panx3 was most likely in the ER (Fig. 2D, d, e). There was no staining signal for Panx3 in undifferentiated ATDC5 cells (Fig. 2D, a). We also examined the expression and localization of Panx3 in pooled stable Panx3-transfected ATDC5 cells (Fig. 3A, B). In these cells, Panx3 mRNA and protein were strongly expressed in an undifferentiated condition. Both anti-Panx3 and anti-V5 antibodies detected the recombinant protein as a single band of about 49 kDa, corresponding to the predicted molecular weight of the Panx3-V5-His fusion protein (Fig. 3A). The immunohistochemistry of Panx3-transfected ATDC5 cells showed that both anti-Panx3 and anti-V5 antibodies strongly stained the plasma membranes (Fig. 3B). Some Panx3 signals were also observed in the endoplasmic reticulum (ER) since ER-

Tracker Red, which had been transiently transfected with the Panx3 expression vector containing a GFP tag, revealed that Panx3 was co-localized with an endoplasmic reticulum (ER) marker. This indicates that the localization of Panx3 was most likely in the ER (Fig. 3C).

Panx3 promotes ATDC5 and N1511 cell differentiation— We next examined whether the overexpression of Panx3 affects ATDC5 cell differentiation. Panx3-transfected ATDC5 cells were cultured under the differentiation condition in the presence of insulin. The expression of chondrocyte marker genes for *Col2a1*, aggrecan (*Agc1*), and *Col10a1* increased by 2.8-, 2.2-, and 5.1-fold, respectively, compared with control pEF1-transfected cells 8 days after induction (Fig. 4A, left panel). The *Panx3* mRNA levels in the Panx3-transfected cells were ~100-fold higher than those in the control pEF1-ATDC5 cells at day 8-induction. At day 16, after induction, the expression of both *Agc1* and *Col10a1* in Panx3-transfected cells was still higher than that of the control cells (Fig. 4A). *Panx3* mRNA in the transfected cells at day 16 was increased by about 2-fold, when its level was normalized with the level of control pEF1-transfected cells. The large decrease in the relative ratio of *Panx3* mRNA levels at day 16 compared to day 8 is due to the endogenous *Panx3* mRNA levels increasing substantially from day 8 to day 16 as shown in Fig. 2A. The actual *Panx3* mRNA levels did not decrease in Panx3-transfected ATDC5 cells during differentiation. Alcian blue staining, often used to stain proteoglycans in cartilage, was also increased in nodules of Panx3-transfected cells compared to the control cells (Fig. 4B). We also examined the expression of chondrogenic marker genes in transiently Panx3-transfected N1511 cells with during differentiation in the presence of insulin and BMP-2 (Fig. 4C). At day 3, the expression of *Col2a1* and *Agc1* mRNA was stimulated in the transfected cells compared to the control pEF1-transfected cells, whereas *Col10a1* mRNA levels was very low in both control pEF1- and Panx3-transfected cells. In day 4, *Col10a1* mRNA was induced in control cells and its expression levels were promoted in Panx3-transfected cells. The total *Panx3* mRNA levels, including exogenous and endogenous *Panx3* mRNA, did not change at day 3 or day 4. Taken together, these results indicate that Panx3 expression promoted chondrogenic cell differentiation.

Suppression of endogenous Panx3 expression inhibits cell differentiation— To analyze the endogenous Panx3 function in ATDC5 cell differentiation, we knocked down Panx3 expression using Panx3 shRNA. We transfected the Panx3 shRNA expression vector into ATDC5 cells. The resulting stably transfected cells were pooled and induced to differentiate in the presence of insulin. After 8 days in culture, the expression of Panx3 was substantially reduced at both the RNA and protein levels, compared with empty vector-transfected cells (Fig. 5A). *Panx3* mRNA was found to be downregulated by ~70% in Panx3 shRNA-transfected cells compared with the controls. In addition, the expression of mRNA for *Col2a1*, *Agc1*, and *Col10a1* in the shRNA-transfected cells was reduced by 50%, 64%, and 15%, respectively (Fig. 5B). Similarly, Alcian blue staining was reduced to 40% of the control cell level at 16 days in culture (Fig. 5C). Similarly, N1511 cell differentiation was inhibited by Panx3 shRNA transfection (data not shown).

To eliminate the possibility of off-target inhibitory effects of shPanx3 on cell differentiation, we used two different types of siRNA for Panx3. Both Panx3 siRNA-1 and -2 inhibited the expression of *Col2a1* and *Col10a1* in ATDC5 cells (Fig. 5D). We also tested these siRNA in primary chondrocytes prepared from cartilage of neonatal mice. Panx3 siRNA-1 and -2 inhibited the expression of *Col10a1*, but not *Col2a1* (Fig. 5E). This may be because primary chondrocytes are a mixture of different chondrocytes in varying stages of differentiation. The suppression of endogenous Panx3 did not affect *Col2a* – expressing chondrocytes, but inhibited differentiation to hypertrophic *Col10a1*-expressing chondrocytes. These results indicate that the suppression of endogenous Panx3 expression inhibited chondrocyte differentiation.

Panx3 inhibits PTH-induced cell proliferation— It has been reported that the expression of connexins such as Cx43, Cx32, and Cx26 inhibits tumor cell growth (27,28). Panx3 may have similar cell growth inhibitory activity, thereby promoting ATDC5 cell differentiation. Because PTH/PTHrP promotes chondrocyte proliferation, we examined Panx3 activity in PTH-mediated ATDC5 cell proliferation. Three days after the addition of PTH, we found that the number of control ATDC5 cells had increased in a dose-responsive manner and that the maximum cell number was reached at 10 nM PTH (Fig. 6). However, the number of Panx3-transfected ATDC5 cells was reduced in response to increasing amounts of PTH compared with the control cells (Fig. 6A). The endogenous PTHrP mRNA levels remained the same in Panx3- and control pEF1-transfected ATDC5 cells, under either proliferation or differentiation conditions (supplemental Fig. 1). PTH/PTHrP receptor (PPR) was induced during differentiation but its expression levels were similar in pEF- and Panx3-transfected cells (supplemental Fig. 1). These results suggest that endogenous PPR and PTHrP did not affect the proliferation and differentiation results. This reduced proliferation activity in Panx3-transfected cells with PTH was blocked by anti-Panx3 antibody, but not control IgG (Fig. 6B). These results suggest that Panx3 inhibits PTH-mediated cell proliferation.

Panx3 reduces intracellular cAMP and ATP levels— Because PTH/PTHrP stimulates the proliferation of chondrocytes through activation of the cAMP pathway (2), we examined the intracellular level of cAMP in Panx3-transfected ATDC5 cells under proliferation conditions (Fig. 7A). In the absence of PTH, the intracellular cAMP level was approximately 10% less in Panx3-transfected cells than in control pEF1-transfected cells. The addition of PTH increased the cAMP level within 10 min by 1.7-fold in pEF1-transfected cells. In contrast, Panx3-transfected cells demonstrated only a 1.2-fold induction by PTH. This reduced induction of the cAMP levels in Panx3-transfected cells was reversed to normal levels by addition of anti-Panx3 antibody, but not by control IgG (Fig. 7A). These data suggest that Panx3 inhibited PTH-mediated proliferation of ATDC5 cells by reducing intracellular cAMP levels.

This result may be due to Panx3 functioning as a hemichannel, releasing ATP to the extracellular space, and thus decreasing the intracellular cAMP level. To examine the hemichannel activity of Panx3, pEF1- and Panx3-transfected ATDC5 cells were treated with PTH, then the release of ATP into the culture medium was measured (Fig. 7B). Panx3-transfected cells exhibited an elevated ATP release that reached a maximum level at 2 min, and then gradually decreased with time. A similar release was not observed in control pEF1-transfected cells. In the presence of a high concentration of potassium glutamate (KGlu), which depolarizes the cell membrane, ATP was released from Panx3-transfected ATDC5 cells (Fig. 7B). A function-blocking antibody specific to the extracellular domain of Panx3 inhibited this ATP efflux (Fig. 7C). This antibody inhibition was blocked by the Panx3 peptide, which was used to raise the Panx3 antibody as an antigen in a dose-dependent manner, whereas its scrambled peptide and control IgG did not affect the antibody inhibition. These results suggest that the Panx3 hemichannel is one of the major ATP release channels.

Panx3 inhibits PTH-induced CREB phosphorylation— We next examined the activation of CREB, which is a downstream molecule of the PTH/PTHrP-cAMP-PKA pathway in chondrocytes (10,29). CREB reached its maximum phosphorylation level at 30 min after PTH treatment in the control pEF1-transfected ATDC5 cells. In Panx3-transfected cells, CREB phosphorylation was significantly reduced (Fig. 8A). The reduced CREB phosphorylation in Panx3-transfected cells was blocked by anti-Panx3 antibody, but not by IgG (Fig. 8B). Taken together, these results suggest that Panx3

inhibits PTH/PTHrP-cAMP-PKA signaling in ATDC5 cells.

DISCUSSION

In this study, we utilized a bioinformatics approach to search for a gap junction protein involved in cartilage development. We found that *Panx3* mRNA was preferentially expressed in a transitional stage between proliferative chondrocytes and terminally differentiated hypertrophic chondrocytes in developing growth plates. This suggests that Panx3 plays a role in the switch from proliferation to differentiation in these chondrocytes. To assess Panx3 action in chondrocyte differentiation, we used a chondrogenic cell lines ATDC5 and N1511, which can be induced to differentiate into chondrocyte phenotypes. *Panx3* mRNA expression was induced during differentiation ATDC5 and N1511 cells (Fig. 2). We demonstrated that the expression of Panx3 promoted differentiation of ATDC5 and N1511 cells (Fig. 4). In contrast, the inhibition of endogenous Panx3 expression through Panx3 shRNA and siRNA reduced differentiation of these cells and primary chondrocytes (Fig. 5 and data not shown) These results suggest that Panx3 regulates chondrogenic cell differentiation.

PTH/PTHrP functions to keep chondrocytes proliferating and to delay hypertrophic chondrocyte differentiation. Both PTHrP-deficient mice and PTH/PTHrP receptor-deficient mice have similar growth plate abnormalities—reduced numbers of chondrocytes and premature hypertrophic differentiation—indicating that PTHrP signals primarily through the PTH/PTHrP receptor in the growth plate (3,5). We found that PTH increased proliferation of ATDC5 cells in culture, but this PTH activity was reduced in Panx3-transfected ATDC5 cells (Fig. 6). There was no significant difference in cell proliferation activity between untransfected and Panx3-transfected ATDC5 cells in the absence of PTH, indicating that the inhibitory activity of Panx3 for cell proliferation is dependent on PTH. The interaction of PTH/PTHrP with the PTH/PTHrP receptor (PPR) promotes the activation of multiple heteromeric G proteins, including G_s, which can activate adenylyl cyclase (AC), and G_q, which can activate phospholipase C/protein kinase C (PLC/PKC), and G_q, whose action occurs opposite the G_s pathway (30,31). The PTH-induced activation of G_s leads to the cascade activation of downstream molecules, specifically the activation of AC, an increase in cAMP levels, the activation of PKA, and the phosphorylation of CREB. The activation of CREB induces the expression of genes required for cell proliferation (Fig. 9).

We found that Panx3 expression in ATDC5 cells promoted ATP release from the cytoplasm to the extracellular space, and this ATP release was inhibited by a function-blocking anti-Panx3 antibody, suggesting that Panx3 plays a specific role in the release of ATP (Fig. 7B, C). The activity of Panx3 as a hemichannel for ATP release would explain the reduced intracellular cAMP levels in Panx3-expressing ATDC5 cells treated with PTH, since ATP is converted to cAMP by AC (32). Thus it is conceivable that Panx3-promoted ATP release to the extracellular space results in the reduction of intracellular cAMP, leading to the inhibition of PTH-induced cell proliferation. Panx3 activity in ATDC5 cells as an ATP-release channel is consistent with recent reports that Panx1 can form a hemichannel for stress-sensitive ATP permeability in oocytes and erythrocytes (19,33).

ATP secreted into the pericellular environment affects a variety of cellular processes. Recently, upregulation of Panx1 has been reported in macrophages stimulated by endotoxin lipopolysaccharide. This treatment mediates large-pore formation of the ATP-gated $P2X_7Rs$ receptor, which leads to interleukin-1 release from the activated macrophage (34). The interaction of ATP with P2 receptors reportedly increases the concentration of intracellular Ca^{2+} in chondrocytes through G_q (35). ATP released into the extracellular space through Panx3 hemichannels at the early differentiation stage may re-enter the cytoplasm through purinergic receptors such as P2Y and P2X and promote differentiation. It is also possible that Panx3 may function as a Ca^{2+} channel in the ER and increase intracellular Ca^{2+} levels for chondrocyte

maturation.

Although Panx3 mRNA is expressed strongly by prehypertrophic chondrocytes, the Panx3 protein is found in both prehypertrophic and hypertrophic chondrocytes (Fig. 1). We did not detect Panx1 or Panx2 in developing growth plates with in situ hybridization (data not shown). Panx1, but not Panx2, was expressed very weakly in ATDC5 cells, but was not induced during ATDC5 cell differentiation (data not shown). Connexin 43 is expressed in condensing mesenchymal cells in the primordial cartilage, and also in articular chondrocytes and osteoblasts. Connexin 43 has been shown to form functional gap junctions capable of sustaining the propagation of intercellular Ca^{2+} waves in articular chondrocyte culture (36) and to regulate BMP-2-mediated chondrogenic differentiation in chick mesenchyme micromass culture (37). Many mutations in the connexin 43 gene have been identified in association with oculodentodigital dysplasia (38,39), which is characterized by syndactyly of the hands and feet, hypoplasia of the middle phalanges, and abnormal craniofacial elements. However, connexin-deficient mice do not exhibit any of the gross abnormalities of chondrocyte differentiation, but they do have mineralization defects (40). Immunostaining of developing growth plates revealed that connexin 43 was not expressed in prehypertrophic and hypertrophic chondrocytes, but it was expressed in osteoblasts (data not shown). These connexin 43 expression patterns are consistent with the skeletal phenotype of connexin43-deficient mice. Thus, Panx3 is likely the major gap junction protein in cartilage.

In conclusion, we demonstrated that Panx3 is uniquely expressed in prehypertrophic and hypertrophic chondrocytes and that it promotes the chondrogenic differentiation of ATDC5 cells, at least in part through its hemichannel activity. Panx3 inhibits PTH-induced ATDC5 cell proliferation and mediates intracellular ATP release into the extracellular space, which in turn leads to a reduction in cAMP/PKA signaling, resulting in decreased proliferation and increased differentiation. Our findings suggest that Panx3 is a regulator of the switching mechanism behind the transition of chondrocytes from a proliferative state to a postmitotic state and that it is required for chondrocyte differentiation.

REFERENCES

1. Kronenberg, H. M. (2003) *Nature* **423**, 332-336
2. Kronenberg, H. M. (2006) *Ann N Y Acad Sci* **1068**, 1-13
3. Karaplis, A. C., Luz, A., Glowacki, J., Bronson, R. T., Tybulewicz, V. L., Kronenberg, H. M., and Mulligan, R. C. (1994) *Genes Dev* **8**, 277-289
4. Miao, D., He, B., Karaplis, A. C., and Goltzman, D. (2002) *J Clin Invest* **109**, 1173-1182
5. Lanske, B., Karaplis, A. C., Lee, K., Luz, A., Vortkamp, A., Pirro, A., Karperien, M., Defize, L. H., Ho, C., Mulligan, R. C., Abou-Samra, A. B., Juppner, H., Segre, G. V., and Kronenberg, H. M. (1996) *Science* **273**, 663-666
6. Weir, E. C., Philbrick, W. M., Amling, M., Neff, L. A., Baron, R., and Broadus, A. E. (1996) *Proc Natl Acad Sci U S A* **93**, 10240-10245
7. Schipani, E., Lanske, B., Hunzelman, J., Luz, A., Kovacs, C. S., Lee, K., Pirro, A., Kronenberg, H. M., and Juppner, H. (1997) *Proc Natl Acad Sci U S A* **94**, 13689-13694
8. Abou-Samra, A. B., Juppner, H., Force, T., Freeman, M. W., Kong, X. F., Schipani, E., Urena, P., Richards, J., Bonventre, J. V., Potts, J. T., Jr., and et al. (1992) *Proc Natl Acad Sci U S A* **89**, 2732-2736
9. Singh, A. T., Gilchrist, A., Voyno-Yasenetskaya, T., Radeff-Huang, J. M., and Stern, P. H. (2005) *Endocrinology* **146**, 2171-2175
10. Beier, F., Ali, Z., Mok, D., Taylor, A. C., Leask, T., Albanese, C., Pestell, R. G., and LuValle, P. (2001) *Mol Biol Cell* **12**, 3852-3863
11. Beier, F., and LuValle, P. (2002) *Mol Endocrinol* **16**, 2163-2173

12. Panchin, Y., Kelmanson, I., Matz, M., Lukyanov, K., Usman, N., and Lukyanov, S. (2000) *Curr Biol* **10**, R473-474
13. Baranova, A., Ivanov, D., Petrash, N., Pestova, A., Skoblov, M., Kelmanson, I., Shagin, D., Nazarenko, S., Geraymovych, E., Litvin, O., Tiunova, A., Born, T. L., Usman, N., Staroverov, D., Lukyanov, S., and Panchin, Y. (2004) *Genomics* **83**, 706-716
14. Vogt, A., Hormuzdi, S. G., and Monyer, H. (2005) *Brain Res Mol Brain Res* **141**, 113-120
15. Penuela, S., Bhalla, R., Gong, X. Q., Cowan, K. N., Celetti, S. J., Cowan, B. J., Bai, D., Shao, Q., and Laird, D. W. (2007) *J Cell Sci* **120**, 3772-3783
16. Penuela, S., Celetti, S. J., Bhalla, R., Shao, Q., and Laird, D. W. (2008) *Cell Commun Adhes* **15**, 133-142
17. Wang, X. H., Streeter, M., Liu, Y. P., and Zhao, H. B. (2009) *J Comp Neurol* **512**, 336-346
18. Bruzzone, R., Hormuzdi, S. G., Barbe, M. T., Herb, A., and Monyer, H. (2003) *Proc Natl Acad Sci U S A* **100**, 13644-13649
19. Bao, L., Locovei, S., and Dahl, G. (2004) *FEBS Lett* **572**, 65-68
20. Vanden Abeele, F., Bidaux, G., Gordienko, D., Beck, B., Panchin, Y. V., Baranova, A. V., Ivanov, D. V., Skryma, R., and Prevarskaya, N. (2006) *J Cell Biol* **174**, 535-546
21. Atsumi, T., Miwa, Y., Kimata, K., and Ikawa, Y. (1990) *Cell Differ Dev* **30**, 109-116
22. Kamiya, N., Jikko, A., Kimata, K., Damsky, C., Shimizu, K., and Watanabe, H. (2002) *J Bone Miner Res* **17**, 1832-1842
23. Williams, J. A., Kondo, N., Okabe, T., Takeshita, N., Pilchak, D. M., Koyama, E., Ochiai, T., Jensen, D., Chu, M. L., Kane, M. A., Napoli, J. L., Enomoto-Iwamoto, M., Ghyselinck, N., Chambon, P., Pacifici, M., and Iwamoto, M. (2009) *Dev Biol* **328**, 315-327
24. Shukunami, C., Ohta, Y., Sakuda, M., and Hiraki, Y. (1998) *Exp Cell Res* **241**, 1-11
25. Nakamura, K., Shirai, T., Morishita, S., Uchida, S., Saeki-Miura, K., and Makishima, F. (1999) *Exp Cell Res* **250**, 351-363
26. Watanabe, H., de Caestecker, M. P., and Yamada, Y. (2001) *J Biol Chem* **276**, 14466-14473
27. Kumar, N. M., and Gilula, N. B. (1996) *Cell* **84**, 381-388
28. Yamasaki, H., and Naus, C. C. (1996) *Carcinogenesis* **17**, 1199-1213
29. Ionescu, A. M., Schwarz, E. M., Vinson, C., Puzas, J. E., Rosier, R., Reynolds, P. R., and O'Keefe, R. J. (2001) *J Biol Chem* **276**, 11639-11647
30. Bringhurst, F. R., Juppner, H., Guo, J., Urena, P., Potts, J. T., Jr., Kronenberg, H. M., Abou-Samra, A. B., and Segre, G. V. (1993) *Endocrinology* **132**, 2090-2098
31. Schwindinger, W. F., Fredericks, J., Watkins, L., Robinson, H., Bathon, J. M., Pines, M., Suva, L. J., and Levine, M. A. (1998) *Endocrine* **8**, 201-209
32. Cooper, D. M. (2003) *Biochem J* **375**, 517-529
33. Locovei, S., Wang, J., and Dahl, G. (2006) *FEBS Lett* **580**, 239-244
34. Pelegrin, P., and Surprenant, A. (2006) *Embo J* **25**, 5071-5082
35. Kaplan, A. D., Kilkenny, D. M., Hill, D. J., and Dixon, S. J. (1996) *Endocrinology* **137**, 4757-4766
36. Tonon, R., and D'Andrea, P. (2000) *J Bone Miner Res* **15**, 1669-1677
37. Zhang, W., Green, C., and Stott, N. S. (2002) *J Cell Physiol* **193**, 233-243
38. Richardson, R., Donnai, D., Meire, F., and Dixon, M. J. (2004) *J Med Genet* **41**, 60-67
39. Kjaer, K. W., Hansen, L., Eiberg, H., Leicht, P., Opitz, J. M., and Tommerup, N. (2004) *Am J Med Genet A* **127A**, 152-157
40. Lecanda, F., Warlow, P. M., Sheikh, S., Furlan, F., Steinberg, T. H., and Civitelli, R. (2000) *J Cell Biol* **151**, 931-944

FOOTNOTES

This work was supported by the Intramural Research Program of the National Institute of Dental and Craniofacial Research, NIH (Y.Y.), a grant-in-aid (20791583 to T.I.) for Research Fellows from the Japan Society for the Promotion of Science and a grant-in-aid (20679006 for S.F) from the Ministry of Education, Science, and Culture of Japan.

ACKNOWLEDGEMENT

We thank Dr. Masahiro Iwamoto for plasmid Hist1h4c, and Dr. Motomi Iwamoto and Dr. Hideto Watanabe for N1511 cells.

FIGURE LEGENDS

Figure 1. Expression of Panx3 in E16.5 growth plates. (A) *In situ* hybridization. Panx3 mRNA was expressed in prehypertrophic chondrocytes, perichondrium, and osteoblasts. Antisense *Panx3* (a); Sense *Panx3* (b); *Ihh* (c); *Col2a1* (d); Col10a1 (e); *Hist1h4c* (f). (B) Immunostaining with anti-Panx3 antibody (red) and Hoechst nuclear staining (blue). Magnified view of the areas (a) marked by the square in (b).

Figure 2. Expression of Panx3 in differentiating ATDC5 and N1511 cells. (A) mRNA expression in differentiating ATDC5 cells. ATDC5 cells were cultured with 10 μg/ml of insulin. Total RNA was extracted from cells on the indicated days after insulin treatment and analyzed with Real-time RT-PCR. In differentiating ATDC5 cells, *Panx3, Col2a1*, and *Col10a1* were strongly induced. *GAPDH*, glyceraldehyde-3-phosphate dehydrogenase, was used as a control. (B) mRNA expression in differentiating N1511 cells. N1511 cells were cultured with 1μM insulin, 100 ng/ml rhBMP-2 and 50μg/ml ascorbic acid for differentiation. Panx3 was also progressively induced in differentiating N1511 cells. HPRT, hypoxanthine phophoribosyltransferase, was used as a control. (C) Expression of Panx3 protein in undifferentiated (lane 1) and differentiated ATDC5 cells (lane 2). ATDC5 cells were treated with or without insulin for 20 days and cell extracts were analyzed by Western blotting using Panx3 antibody. Panx3 protein was induced in differentiated ATDC5 cells. (D) Immunostaining with anti-Panx3 antibody (red), endoplasmic reticulum (ER) maker (green), Calnexin, and Hoechst nuclear staining (blue). In differentiating ATDC5 cells, endogenous Panx3 was observed in the cell membrane, cell processes and ER (d, e, and f), but not in undifferentiated cells (a and c).

Figure 3. Panx3 expression in Panx3-transfected ATDC5 cells. ATDC5 cells were stably transfected with the control empty vector (pEF1) or the Panx3 expression vector (pEF1/Panx3). (A) Expression of Panx3 mRNA and protein. Pooled transfectants were analyzed by (a) RT-PCR and (b) Western blotting using anti-Panx3 and -V5 antibodies. (B) Immunostaining of Panx3-transfected ATDC5 cells using anti-Panx3 (red) and -V5 (blue) antibodies. Fluorescent confocal images showed that the staining signals of Panx3 and V5 antibodies were co-localized in the cell membrane, cell-cell junction, and organelles. No staining of either Panx3 or V5 antibodies was observed in control pEF1-transfected ATDC5 cells. (C) Co-localization of Panx3-GFP and ER-Tracker Red. ATDC5 cells were transiently transfected with Panx3-pcDNA-GFP or pcDNA3.1-GFP-TOPO (control) for 2 days. Panx3-GFP was co-localized with ER-Tracker Red, indicating the presence of Panx3 in ER.

Figure 4. Panx3 promotes chondrogenic differentiation of ATDC5 and N1511 cells. (A) Differentiation of ATDC 5 cells. Pooled ATDC5 cells stably transfected with either control pEF1 or pEF1/Panx3 were cultured with 10 μg/ml of insulin. Total RNA was extracted at 8 days and 16 days after insulin treatment and analyzed by real-time RT-PCR. The expression of chondrogenic marker genes for Col2a1, Agc1, and Col10a1 was stimulated in Panx3-transfected ATDC5 cells

compared with that in control cells. The expression level of an individual gene in control pEF1-transfected cells was set as 1.0 and compared it with the level of each gene in Panx3-transfected cells for each day 8 and day 18. The exogenous Panx3 levels were the same but endogenous Panx3 levels were strongly increased from day 8 to day 16. As results, the ratio at day 16 was less than that in day 8. (B) Alcian blue staining of ATDC5 cells. After 16 days of culture, Alcian blue staining was performed. Alcian blue staining was increased in Panx3-transfected ATDC5 cells compared to that in pEF1-transfected ATDC5 cells. Scale bar, 200 μm. (C) Differentiation of N1511 cells. N1511 cells were transfected with either control pEF1 or pEF1/Panx3, were cultured with 1μM insulin, 100 ng/ml rhBMP-2 and 50μg/ml ascorbic acid for 3 days and 4 days. Similar to the results of ATDC5 cells, chondrogenic maker genes expression was stimulated by Panx3. Statistical analysis was performed using analysis of variance (*P<0.01).

Figure 5. Inhibition of ATDC5 cell differentiation by Panx3 shRNA. Pooled ATDC5 cells stably transfected with either control vector (Mock) or Panx3 shRNA vector were cultured with 10 μg/ml insulin. (A) Reduced expression of endogenous Panx3. Total RNA and protein were prepared from cells after 8 days of culture and analyzed through (a) RT-PCR and (b) Western blotting using anti-Panx3 antibody. Panx3 expression was reduced in Panx3 shRNA-transfected ATDC5 cells. (B) Reduced expression of chondrogenic marker genes. Total RNA was prepared from cells after 8 days of culture and analyzed by real-time RT-PCR. Expression of *Col2a1, Agc1*, and *Col10a1* was reduced in Panx3 shRNA-transfected ATDC5 cells. (C) Alcian blue staining. After 16 days of culture, Alcian blue staining was performed. Alcian blue staining was reduced in Panx3 shRNA-transfected cells. Scale bar, 200 μm. Statistical analysis was performed using analysis of variance (*P<0.01). (D) Reduced expression of Col2a1 and Col10a1 by Panx3 siRNA in ATDC5 cells. ATDC5 cells transfected with control siRNA, Panx3 siRNA-1 or Panx3 siRNA-2, were cultured with 100 ng/ml BMP-2 for 8 days. Expressions of Panx3, Col2a1 and Col10a1 were analyzed by real time PCR methods. Expression of Col2a1 and Col10a1 was reduced in Panx3 siRNA-transfected ATDC5 cells. (E) Reduced expression of Col10a1 but not Col2a1 by Panx3 siRNA in primary chondrocytes. Primary chondrocytes transfected with control siRNA, Panx3 siRNA-1 or Panx3 siRNA-2, were cultured with 100 ng/ml BMP-2 for 2 days. Expression of Panx3, Col2a1 and Col10a1, were analyzed by real time PCR methods. Expression of Panx3 and Col10a1, but not Col2a1, was reduced in Panx3 siRNA-transfected primary chondrocytes. Statistical analysis was performed using analysis of variance (*P<0.01).

Figure 6. Inhibition of PTH-promoted cell proliferation by Panx3. (A) The Panx3- and pEF1-transfected cells were incubated in the presence of various amounts of PTH. Cell numbers were counted after 3 days of culture. The number of Panx3-transfected cells was reduced compared with the control cells. (B) Panx3 antibody, but not IgG, restored PTH-promoted cell proliferation in Panx3-transfected cells. Statistical analysis was performed using analysis of variance (**P<0.02, *P<0.01).

Figure 7. Reduced cAMP levels and increased ATP efflux in Panx3-transfected ATDC5 cells. (A) Intracellular cAMP level. Panx3- and pEF1-transfected ATDC5 cells were cultured with 10 μg/ml of insulin for 1 week. The cells were incubated with anti-Panx3, IgG or without them for 30 min, and then exposed to PTH at 100 nM for 10 min and analyzed the intracellular cAMP levels. PTH promoted the intracellular cAMP level in control pEF1-transfected cells, whereas this PTH effect was reduced in Panx3-transfected cells. This reduction was blocked by anti-Panx3 antibody but not IgG. (B) Release of ATP. Cells were plated at ~50% confluency in the absence or presence of potassium (KGlu), and ATP levels in the media were measured. ATP release to the extracellular space was increased in Panx3-transfected cells. Left panel: time-course of ATP release after addition of KGlu. Right panel: data at 2 min after addition of KGlu in the right panel were shown in bar graphs. Statistical analysis was performed using analysis of variance (*P<0.01). (C) Inhibition of ATP release by Panx3 antibody. Cells were incubated with anti-Panx3 antibody, Panx3 peptide or IgG for 30 min, and ATP release was measured. The Panx3

antibody inhibited ATP release in Panx3-transfected cells. This inhibition was blocked by various concentrations (0.5 to 5.0 ng/mL) of the Panx3 peptide, but not its scrambled peptide (5.0 ng/mL).

Figure 8. Decrease in phosphorylation of CREB by Panx3. (A) Time-course of CREB phosphorylation. ATDC5 cells were cultured with 10 μg/ml of insulin for 1 week and then treated with PTH (100 nM) for the time indicated. Protein extracts were analyzed by Western blotting using anti-phospho-CREB and anti-CREB antibodies. In control pEF1-transfected cells, the phosphorylation of CREB was strongly induced, whereas in Panx3-transfected cells the phosphorylation levels of CREB were reduced. (B) Restoration of the CREB phosphorylation levels by Panx3 antibody. Cells were preincubated with Panx3 antibody or IgG for 30 min before the stimulation with 100 nM PTH, and then Western blotting using anti-phospho-CREB and anti-CREB antibodies were performed. Panx3 antibody inhibited the reduction of the phosphorylation of CREB in Panx3-transfected cells. *Image J* 1.33u was used to quantify the protein bands.

Figure 9. Role of Panx3 in chondrogenic differentiation. The PTH/PTHrP receptor activates multimeric G proteins. The activation of the Gs subunit leads to the activation of adenylyl cyclase (AC) for cAMP generation from ATP and the subsequent activation of PKA. PKA phosphorylates CREB, which promotes the expression of genes for cell proliferation. Panx3 is expressed in prehypertrophic chondrocytes and it promotes the release of ATP into the extracellular space, which results in a reduction of the intracellular cAMP level and subsequent inhibition of PKA/CREB signaling for cell proliferation. The PTH/PTHrP receptor also activates the G_q subunit and subsequent downstream signaling, such as PKC, to promote differentiation.

Fig. 1

A

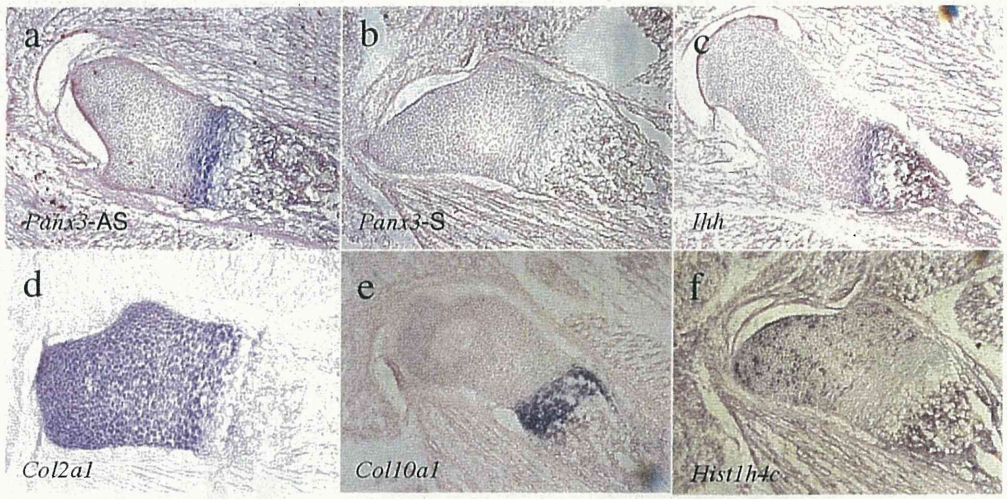

B

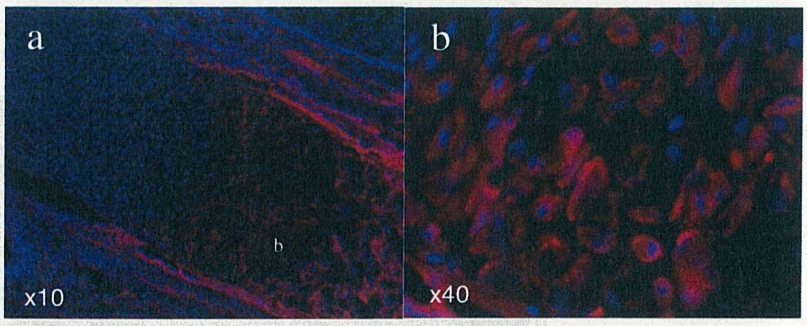

Fig. 2

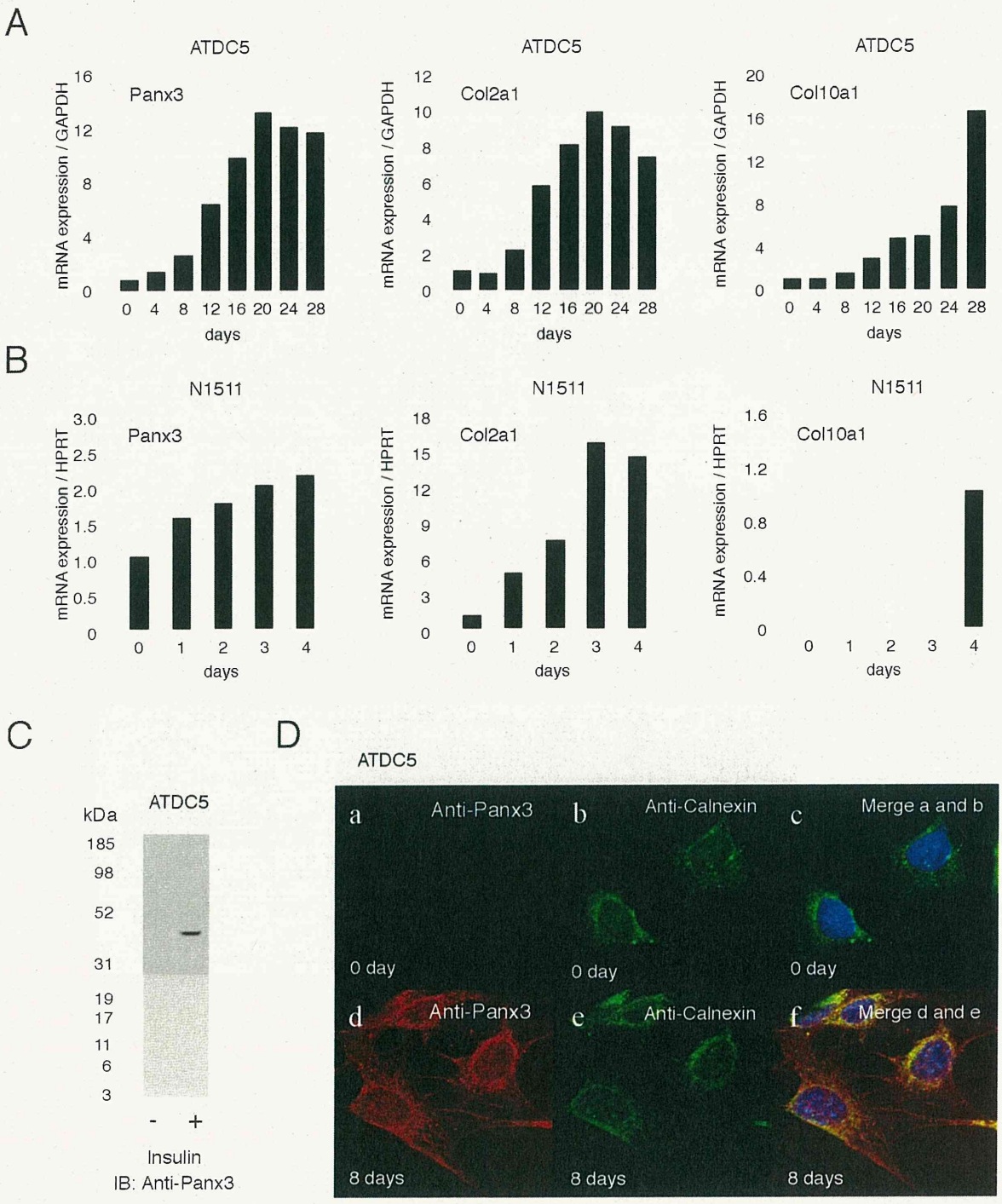

Iwamoto et al.

Fig. 3

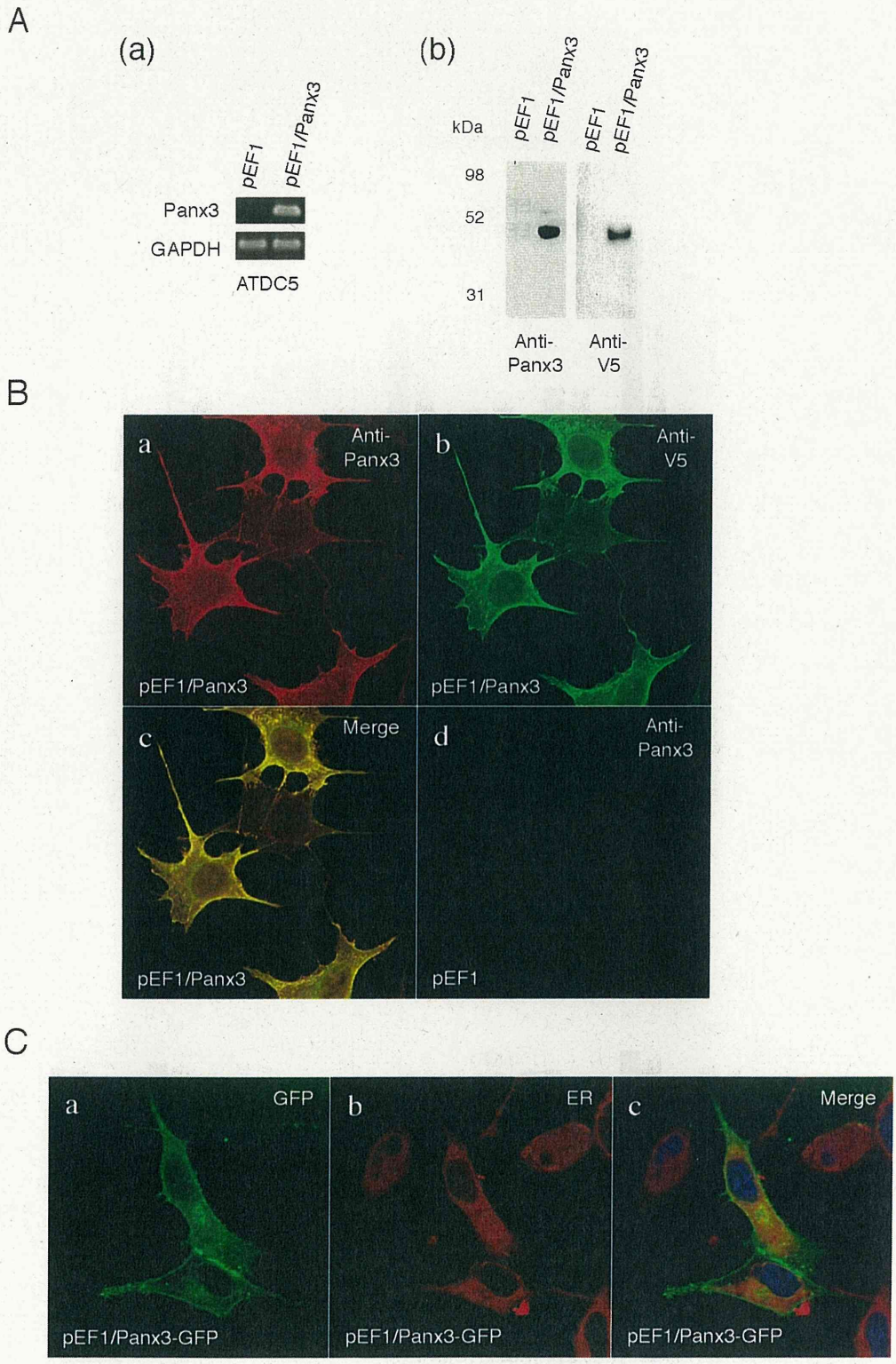

Fig. 4